

Regular article

Finding transition states using reduced potential-energy surfaces

Josep Maria Bofill¹, Josep Maria Anglada²

¹ Departament de Química Orgànica i Centre Especial de Recerca en Química Teòrica, Universitat de Barcelona, c./Martí i Franquès 1, 08028 Barcelona, Catalonia, Spain

² Institut de Investigacions Químiques i Ambientals de Barcelona, CSIC, c./Jordi Girona Salgado 18–26, 08034 Barcelona, Catalonia, Spain

Received: 29 September 2000 / Accepted: 3 January 2001 / Published online: 3 April 2001
© Springer-Verlag 2001

Abstract. We propose a method to locate saddle points that is based on the interplay between the driving coordinate and the restricted quasi-Newton algorithm. The method locates the transition state using a reduced potential-energy surface. The reduced potential-energy surface is characterized by the set of driving coordinates. The proposed algorithm starts at a point on the surface that is slightly perturbed from either reactant or product and, in principle, converges to the transition state. Finally we give a special type of update Hessian matrix formula that should be applied in optimizations carried out on reduced potential-energy surfaces.

Key words: Locating transition states – Saddle points – Restricted quasi-Newton–Raphson algorithm – Update Hessian matrix formula

1 Introduction

Transition-state theory is an approach to study the mechanism and kinetics of chemical reactions. The application of this theory basically consists of locating the reactant, the product, and the corresponding transition state on the potential-energy surface (PES) associated with the elementary reaction under consideration. The reactant and the product are associated with minima, whereas the transition state is associated with a first-order saddle point [1].

The location of a saddle point is an open question; however, there are a set of powerful methods such that in most of the cases the transition state is reached without effort. A good review of methods for locating transition states is given by Schlegel [2].

Using the classification of the algorithms to locate transition states given by Schlegel [2], the coordinate-driving technique combined with quasi-Newton methods

and walking up valleys are the most widely used techniques to find saddle points. In particular, the eigenvector-following approach can be seen as a combination of walking up valleys and quasi-Newton optimization [3, 4, 5, 6, 7, 8, 9, 10, 11, 12, 13].

In the driving-coordinate technique one assumes that the reaction under consideration can be characterized by a coordinate or by a small subset of coordinates. In this way a type of reaction path is obtained by fixing the selected coordinate and minimizing the PES with respect to the remaining coordinates. The maximum energy point of this path is normally very close to the desired transition state; consequently by taking this point and using the eigenvector-following approach convergence to the transition state is achieved in a few steps. The eigenvector-following technique is based on a type of quasi-Newton algorithm such that the Hessian matrix possesses a negative eigenvalue and it is assumed that its associated eigenvector possesses a topological structure very similar to the desired transition vector. This fact combined with the restricted step is the basis of the eigenvector-following technique.

The difficulty in the eigenvector-following algorithm appears when the starting point is far from the desired transition state and the Hessian matrix does not possess a single eigenvector with a negative eigenvalue [14]. In this situation one selects an eigenvector and the corresponding eigenvalue is forced to be negative; the rest of the eigenvalues are forced to be positive. On the other hand, the problem associated with the driving-coordinate method resides in the correct selection of the dominant coordinate, otherwise one will obtain a non-continuous path [15, 16, 17, 18, 19].

Taking the advantages of both techniques, the driving coordinate and the eigenvector-following algorithm, we propose a method based on walking up valleys/the eigenvector-following algorithm but with the structure of a driving coordinate. In this way the components of the direction vector for walking up valleys or the eigenvector to follow only are the dominant coordinates of the reaction under study. Recently, a similar technique has been proposed but using the philosophy of the

gradient line reaction path concept [20, 21]. The proposed method is based on the technique of walking up valleys developed by Cerjan and Miller [4] and modified by Culot et al. [12]. We note that the walking up valleys technique is in fact a Newton–Raphson algorithm such that the Hessian matrix is shifted. The shift parameter is evaluated in such a way that the shifted Hessian matrix preserves the desired number of negative eigenvalues and the resulting step falls in a trust region. The trust region is the region where the current quadratic expansion is valid. The so-called rational function optimization (RFO) technique [7] is very close to the walking up valley method, the only difference is that the shift parameter is evaluated as a scalar product between the displacement and gradient vectors.

The article is organized in the following way. In Sect. 2 we briefly present and analyze the driving-coordinate method through the concept of a reduced PES. The mathematical structure of the walking up valley/the eigenvector-following algorithm when used in a reduced PES is described in Sect. 3. An algorithm is also outlined. Finally, in Sect. 4 we present and analyze some examples.

2 The reduced PES

During the evolution of a chemical reaction, some subsets of coordinates present very large changes, whereas for the rest of the coordinates the variation is very small. From this observation we can regard a chemical reaction as a limit system in that some coordinates are associated with the “driving force” of the reaction and the remaining coordinates are in adapted equilibria during the process. An example of this behavior can be seen in the conformational transitions of peptides which are dominated by the changes of some torsional angles [14]. However, we emphasize that many chemical reactions do not occur through this type of path; consequently the evaluation of this path is only to locate the transition state. This model of chemical reaction can be written mathematically as

$$V(\mathbf{q}_r) = \min_{\mathbf{q}_p} E(\mathbf{q}_r, \mathbf{q}_p) , \quad (1)$$

where E is the potential energy, \mathbf{q}_r denotes the subset of “driving force” coordinates, i.e., the coordinates that present the large change in the reaction, and \mathbf{q}_p is the set of coordinates that are “equilibrium-adapted” during all the path. Note that $V(\mathbf{q}_r)$ is the energy of a point on the reduced PES (RPES). On each point of the RPES the \mathbf{q}_p coordinates are a function of the \mathbf{q}_r coordinates. The equilibrium condition is given by the relation

$$(\mathbf{g}_p)_i = \frac{\partial E(\mathbf{q}_r, \mathbf{q}_p)}{\partial p_i} = 0 \quad i = 1, \dots, m , \quad (2)$$

where m is the length or dimension of the \mathbf{q}_p vector. Equations (1) and (2) are the basis of the driving-coordinate method [15, 17, 18, 19]. Now we are looking for an explicit mathematical form of Eq. (1) that can be used for future purposes. In order to do this we write an expression for the potential energy $E(\mathbf{q}_r, \mathbf{q}_p)$ by expanding its $\mathbf{q} = (\mathbf{q}_r, \mathbf{q}_p)$ dependence to second order about \mathbf{q}^0

$$\begin{aligned} E(\mathbf{q}_r, \mathbf{q}_p) - E(\mathbf{q}_r^0, \mathbf{q}_p^0) &\cong Q(\Delta\mathbf{q}_r, \Delta\mathbf{q}_p) \\ &= \begin{bmatrix} (\Delta\mathbf{q}_r^0)^T & (\Delta\mathbf{q}_p^0)^T \end{bmatrix} \begin{pmatrix} \mathbf{g}_r^0 \\ \mathbf{g}_p^0 \end{pmatrix} \\ &\quad + \frac{1}{2} \begin{bmatrix} (\Delta\mathbf{q}_r^0)^T & (\Delta\mathbf{q}_p^0)^T \end{bmatrix} \begin{pmatrix} \mathbf{F}_{rr}^0 & \mathbf{F}_{rp}^0 \\ \mathbf{F}_{pr}^0 & \mathbf{F}_{pp}^0 \end{pmatrix} \begin{pmatrix} \Delta\mathbf{q}_r^0 \\ \Delta\mathbf{q}_p^0 \end{pmatrix} , \quad (3) \end{aligned}$$

where $\Delta\mathbf{q}_i^0 = (\mathbf{q}_i - \mathbf{q}_i^0)$, for $i = r, p$ and

$$(\mathbf{g}_r^0)_i = \left. \frac{\partial E(\mathbf{q}_r, \mathbf{q}_p)}{\partial r_i} \right|_{\mathbf{q}=\mathbf{q}^0} \quad i = 1, \dots, n , \quad (4)$$

$$(\mathbf{F}_{rr}^0)_{ij} = \left. \frac{\partial^2 E(\mathbf{q}_r, \mathbf{q}_p)}{\partial r_i \partial r_j} \right|_{\mathbf{q}=\mathbf{q}^0} \quad i, j = 1, \dots, n , \quad (5)$$

$$(\mathbf{F}_{pp}^0)_{ij} = \left. \frac{\partial^2 E(\mathbf{q}_r, \mathbf{q}_p)}{\partial p_i \partial p_j} \right|_{\mathbf{q}=\mathbf{q}^0} \quad i, j = 1, \dots, m , \quad (6)$$

$$(\mathbf{F}_{rp}^0)_{ij} = \left. \frac{\partial^2 E(\mathbf{q}_r, \mathbf{q}_p)}{\partial r_i \partial p_j} \right|_{\mathbf{q}=\mathbf{q}^0} \quad i = 1, \dots, n; \quad j = 1, \dots, m . \quad (7)$$

Note that $r_i = (\mathbf{q}_r)_i$, $p_i = (\mathbf{q}_p)_i$, \mathbf{g}_p^0 is the \mathbf{g}_p part of the gradient vector evaluated at \mathbf{q}^0 , and the number n is the length or dimension of the \mathbf{q}_r vector. Now we apply the Schur transformation [24] on Eq. (3). The Schur transformation is defined as

$$\begin{aligned} \begin{pmatrix} \mathbf{F}_{rr}^0 & \mathbf{F}_{rp}^0 \\ \mathbf{F}_{pr}^0 & \mathbf{F}_{pp}^0 \end{pmatrix} &= \begin{pmatrix} \mathbf{I}_{rr} & \mathbf{F}_{rp}^0 (\mathbf{F}_{pp}^0)^{-1} \\ \mathbf{0}_{pr} & \mathbf{I}_{pp} \end{pmatrix} \begin{pmatrix} \bar{\mathbf{F}}_{rr}^0 & \mathbf{0}_{rp} \\ \mathbf{0}_{pr} & \mathbf{F}_{pp}^0 \end{pmatrix} \\ &\quad \times \begin{pmatrix} \mathbf{I}_{rr} & \mathbf{0}_{rp} \\ (\mathbf{F}_{pp}^0)^{-1} \mathbf{F}_{pr}^0 & \mathbf{I}_{pp} \end{pmatrix} , \quad (8) \end{aligned}$$

where

$$\bar{\mathbf{F}}_{rr}^0 = \mathbf{F}_{rr}^0 - \mathbf{F}_{rp}^0 (\mathbf{F}_{pp}^0)^{-1} \mathbf{F}_{pr}^0 \quad (9)$$

is the reduced or effective Hessian matrix evaluated at \mathbf{q}^0 . The Schur transformation is not an orthogonal transformation; however, it possesses the following property

$$\begin{aligned} \begin{pmatrix} \mathbf{I}_{rr} & \mathbf{0}_{rp} \\ (\mathbf{F}_{pp}^0)^{-1} \mathbf{F}_{pr}^0 & \mathbf{I}_{pp} \end{pmatrix} \begin{pmatrix} \mathbf{I}_{rr} & \mathbf{0}_{rp} \\ -(\mathbf{F}_{pp}^0)^{-1} \mathbf{F}_{pr}^0 & \mathbf{I}_{pp} \end{pmatrix} \\ = \begin{pmatrix} \mathbf{I}_{rr} & \mathbf{0}_{rp} \\ \mathbf{0}_{pr} & \mathbf{I}_{pp} \end{pmatrix} . \quad (10) \end{aligned}$$

The use of this type of transformation rather than an orthogonal transformation is because the Schur transformation does not mix the two subsets of coordinates (note that in general this is not possible using an orthogonal transformation). Substituting Eq. (8) in Eq. (3) and taking into account Eq. (10) we get

$$Q(\Delta\bar{\mathbf{q}}_r^0, \Delta\bar{\mathbf{q}}_p^0) = (\Delta\bar{\mathbf{q}}_r^0)^T \bar{\mathbf{g}}_r^0 + (\Delta\bar{\mathbf{q}}_p^0)^T \bar{\mathbf{g}}_p^0 + \frac{1}{2} (\Delta\bar{\mathbf{q}}_r^0)^T \bar{\mathbf{F}}_{rr}^0 \Delta\bar{\mathbf{q}}_r^0 + \frac{1}{2} (\Delta\bar{\mathbf{q}}_p^0)^T \mathbf{F}_{pp}^0 \Delta\bar{\mathbf{q}}_p^0, \quad (11)$$

where

$$\Delta\bar{\mathbf{q}}_r^0 = \Delta\mathbf{q}_r^0, \quad (12)$$

$$\Delta\bar{\mathbf{q}}_p^0 = (\mathbf{F}_{pp}^0)^{-1} \mathbf{F}_{pr}^0 \Delta\mathbf{q}_r^0 + \Delta\mathbf{q}_p^0, \quad (13)$$

$$\bar{\mathbf{g}}_r^0 = \mathbf{g}_r^0 - \mathbf{F}_{rp}^0 (\mathbf{F}_{pp}^0)^{-1} \mathbf{g}_p^0, \quad (14)$$

$$\bar{\mathbf{g}}_p^0 = \mathbf{g}_p^0. \quad (15)$$

Now, if we start at a point such that $\mathbf{g}_p^0 = \mathbf{0}_p$ and $\mathbf{g}_r^0 \neq \mathbf{0}_r$ then Eq. (14) is reduced to $\bar{\mathbf{g}}_r^0 = \mathbf{g}_r^0$ and from Eq. (15) $\bar{\mathbf{g}}_p^0 = \mathbf{0}_p$. If under these conditions we minimize $Q(\Delta\bar{\mathbf{q}}_r^0, \Delta\bar{\mathbf{q}}_p^0)$ given in Eq. (11) with respect to $\Delta\bar{\mathbf{q}}_p^0$, we obtain the desired form for the RPES as defined in Eq. (1) as a function of the set of driving coordinates, $\Delta\mathbf{q}_r^0$, up to second order:

$$V^{(2)}(\mathbf{q}_r) = E(\mathbf{q}_r^0, \mathbf{q}_p^0) + (\Delta\mathbf{q}_r^0)^T \mathbf{g}_r^0 + \frac{1}{2} (\Delta\mathbf{q}_r^0)^T \bar{\mathbf{F}}_{rr}^0 \Delta\mathbf{q}_r^0. \quad (16)$$

Since $\Delta\bar{\mathbf{q}}_p^0 = \mathbf{0}_p$, from Eq. (13) we get

$$\Delta\mathbf{q}_p^0 = -(\mathbf{F}_{pp}^0)^{-1} \mathbf{F}_{pr}^0 \Delta\mathbf{q}_r^0. \quad (17)$$

Equation (17) tells us that on the RPES defined by the driving coordinates, the set of adapted coordinates, \mathbf{q}_p , are a function of the set of driving coordinates, \mathbf{q}_r . The relation between both sets of coordinates is linear because the RPES is expanded to second order. An important feature is that since the \mathbf{F}_{pp}^0 matrix is positive-definite it is possible to prove that the number of negative eigenvalues of the full Hessian matrix is equal to the number of negative eigenvalues of the reduced or effective Hessian matrix, $\bar{\mathbf{F}}_{rr}^0$ [25, 26]. Consequently, a stationary-point-character minimum on the RPES is also a stationary-point-character minimum on the full PES; on the other hand, a stationary-point-character first-order saddle point on the RPES is also a stationary point of the same character on the full PES [21, 22].

3 The search for the first-order saddle point on the RPES

3.1 Mathematical basis

The walking up valley algorithm was initially proposed by Cerjan and Miller [4]. The purpose of this method is to find a first-order saddle point by preserving during the search the correct number of negative eigenvalues of the Hessian matrix and in addition to ensure that the current quadratic model is valid in some region of the real PES. This algorithm is an extension of the Levenberg–Marquart technique to locate a minimum on a surface [23].

An algorithm that takes all these features into account should be based on the following Lagrangian function [4]

$$L(\Delta\mathbf{q}_r^0, \Delta\mathbf{q}_p^0, \lambda) = (\Delta\mathbf{q}_r^0)^T \mathbf{g}_r^0 + (\Delta\mathbf{q}_p^0)^T \mathbf{g}_p^0 + \frac{1}{2} \left[(\Delta\mathbf{q}_r^0)^T \quad (\Delta\mathbf{q}_p^0)^T \right] \begin{pmatrix} \mathbf{F}_{rr}^0 & \mathbf{F}_{rp}^0 \\ \mathbf{F}_{pr}^0 & \mathbf{F}_{pp}^0 \end{pmatrix} \begin{pmatrix} \Delta\mathbf{q}_r^0 \\ \Delta\mathbf{q}_p^0 \end{pmatrix} - \frac{1}{2} \lambda \left\{ \left[(\Delta\mathbf{q}_r^0)^T \quad (\Delta\mathbf{q}_p^0)^T \right] \begin{pmatrix} \Delta\mathbf{q}_r^0 \\ \Delta\mathbf{q}_p^0 \end{pmatrix} - R^2 \right\}, \quad (18)$$

where R is the radius of a ball that characterizes the trust region. Now, if we start at a point such that $\mathbf{g}_p^0 = \mathbf{0}_p$ the stationary conditions of the Lagrangian function of Eq. (18) are

$$\begin{pmatrix} \mathbf{0}_r \\ \mathbf{0}_p \end{pmatrix} = \begin{pmatrix} \mathbf{g}_r^0 \\ \mathbf{0}_p \end{pmatrix} + \left[\begin{pmatrix} \mathbf{F}_{rr}^0 & \mathbf{F}_{rp}^0 \\ \mathbf{F}_{pr}^0 & \mathbf{F}_{pp}^0 \end{pmatrix} - \lambda \begin{pmatrix} \mathbf{I}_{rr} & \mathbf{0}_{rp} \\ \mathbf{0}_{pr} & \mathbf{I}_{pp} \end{pmatrix} \right] \begin{pmatrix} \Delta\mathbf{q}_r^0 \\ \Delta\mathbf{q}_p^0 \end{pmatrix}, \quad (19)$$

$$0 = \left[(\Delta\mathbf{q}_r^0)^T \quad (\Delta\mathbf{q}_p^0)^T \right] \begin{pmatrix} \Delta\mathbf{q}_r^0 \\ \Delta\mathbf{q}_p^0 \end{pmatrix} - R^2. \quad (20)$$

From Eq. (19) we obtain the relation between $\Delta\mathbf{q}_p^0$ and $\Delta\mathbf{q}_r^0$; this relation is

$$\Delta\mathbf{q}_p^0 = -(\mathbf{F}_{pp}^0 - \lambda \mathbf{I}_{pp})^{-1} \mathbf{F}_{pr}^0 \Delta\mathbf{q}_r^0. \quad (21)$$

Substituting Eq. (21) in Eq. (18) and taking into account that $\mathbf{g}_p^0 = \mathbf{0}_p$ we obtain the new Lagrangian function, which is only a function of the Lagrangian multiplier λ and $\Delta\mathbf{q}_r^0$:

$$L(\Delta\mathbf{q}_r^0, \lambda) = (\Delta\mathbf{q}_r^0)^T \mathbf{g}_r^0 + \frac{1}{2} (\Delta\mathbf{q}_r^0)^T \times \left[\mathbf{F}_{rr}^0 - \lambda \mathbf{I}_{rr} - \mathbf{F}_{rp}^0 (\mathbf{F}_{pp}^0 - \lambda \mathbf{I}_{pp})^{-1} \mathbf{F}_{pr}^0 \right] \times \Delta\mathbf{q}_r^0 + \frac{1}{2} \lambda R^2. \quad (22)$$

Equation (22) is the Lagrangian function given in Eq. (18) but applied to a RPES. Equation (22) is difficult to evaluate since the quadratic part depends of the Lagrangian multiplier in a complicated way. To deal with this problem we substitute the equality

$$(\mathbf{F}_{pp}^0 - \lambda \mathbf{I}_{pp})^{-1} = (\mathbf{F}_{pp}^0)^{-1} \sum_{k=0}^{\infty} \left[\lambda (\mathbf{F}_{pp}^0)^{-1} \right]^k \quad (23)$$

up to first order with respect to λ in Eq. (22). After some rearrangement one obtains

$$L(\Delta\mathbf{q}_r^0, \lambda) \cong (\Delta\mathbf{q}_r^0)^T \mathbf{g}_r^0 + \frac{1}{2} (\Delta\mathbf{q}_r^0)^T \bar{\mathbf{F}}_{rr}^0 \Delta\mathbf{q}_r^0 - \frac{1}{2} \lambda \left[(\Delta\mathbf{q}_r^0)^T \mathbf{S}_{rr}^0 \Delta\mathbf{q}_r^0 - R^2 \right], \quad (24)$$

where

$$\mathbf{S}_{rr}^0 = \mathbf{I}_{rr} + \mathbf{F}_{rp}^0 (\mathbf{F}_{pp}^0)^{-2} \mathbf{F}_{pr}^0. \quad (25)$$

Note that the \mathbf{S}_{rr}^0 matrix is positive-definite. The stationary conditions of the approximated Lagrangian function given in Eq. (24) are

$$\mathbf{0}_r = \mathbf{g}_r^0 + \left(\bar{\mathbf{F}}_{rr}^0 - \lambda \mathbf{S}_{rr}^0 \right) \Delta \mathbf{q}_r^0, \quad (26)$$

$$0 = (\Delta \mathbf{q}_r^0)^T \mathbf{S}_{rr}^0 \Delta \mathbf{q}_r^0 - R^2. \quad (27)$$

To solve this set of equations (Eqs. 26, 27) we make the following matrix transformations: $\Delta \bar{\mathbf{q}}_r^0 = (\mathbf{S}_{rr}^0)^{1/2} \Delta \mathbf{q}_r^0$, $\bar{\mathbf{g}}_r^0 = (\mathbf{S}_{rr}^0)^{-1/2} \mathbf{g}_r^0$, and $\bar{\mathbf{F}}_{rr}^0 = (\mathbf{S}_{rr}^0)^{-1/2} \mathbf{F}_{rr}^0 (\mathbf{S}_{rr}^0)^{-1/2}$. With these transformations the stationary conditions (Eqs. 26, 27) take the usual form

$$\mathbf{0}_r = \bar{\mathbf{g}}_r^0 + \left(\bar{\mathbf{F}}_{rr}^0 - \lambda \mathbf{I}_{rr} \right) \Delta \bar{\mathbf{q}}_r^0, \quad (28)$$

$$0 = \left(\Delta \bar{\mathbf{q}}_r^0 \right)^T \Delta \bar{\mathbf{q}}_r^0 - R^2. \quad (29)$$

These sets of equations are solved in the normal way [4, 6, 7, 8, 12, 13]. From these equations it is possible to show that there are a maximum of $n + 1$ and a minimum of two λ parameters; consequently it is necessary to have a criterium in order to select the adequate parameter. The λ parameter shifts the Hessian matrix: the effect of this shift is to preserve or achieve the correct structure of the shifted Hessian matrix in such a way that the resulting displacement vector, $\Delta \mathbf{q}_r^0$, possesses the correct direction to locate the desired transition state [7, 8, 12, 13, 27]. In the RPES model the parameter λ should be selected in a way that the \mathbf{F}_{pp}^0 matrix preserves its positive character during all the search. On the other hand, the effect of the parameter λ on the reduced or effective Hessian matrix, $\bar{\mathbf{F}}_{rr}^0$, depends on the character, the number of negative and positive eigenvalues, of this effective Hessian matrix. Near a stationary-point-type minimum the $\bar{\mathbf{F}}_{rr}^0$ matrix is positive-definite; in this situation λ is selected such that the resulting shifted effective or reduced Hessian matrix is totally negative-definite, in others words all its eigenvalues are negative. In this case the computed displacement vector, $\Delta \mathbf{q}_r^0$, is ascending in all the directions that define the RPES. In this situation looking at the full PES, the direction of the $\Delta \mathbf{q}_r^0$ vector is monitored by both the subset of the \mathbf{q}_r coordinates and the subset of the \mathbf{q}_p coordinates. These \mathbf{q}_p coordinates follow the \mathbf{q}_r coordinates according to Eq. (21). Far from the minimum region and owing to the continuity of the Hessian matrix function with respect to the coordinates, there is a point on this continuous walk such that the corresponding reduced or effective Hessian matrix possesses a negative eigenvalue. In this case λ is selected in such a way that the resulting shifted, reduced Hessian matrix possesses a negative eigenvalue and only one. In others words we select the λ that preserves the character of the reduced or effective Hessian matrix in order to converge to a first-order saddle point. Note that under this requirement the full Hessian matrix has a negative eigenvalue since the \mathbf{F}_{pp}^0 matrix is positive-definite during all this walk. Sometimes, in the region where the reduced or effective Hessian matrix, $\bar{\mathbf{F}}_{rr}^0$, already possesses a negative eigenvalue in the next step, this matrix has two negative eigenvalues; in this case λ is

selected in a way that the shifted reduced Hessian matrix has a negative eigenvalue. All these previous considerations were taken from the analysis of the RFO method to locate first-order saddle points [7, 12, 13, 27].

The trust radius defines the validity region of the current quadratic model around the current point with respect to the real PES expanded around this point. Since both the real surface and the quadratic model change during the search process it is necessary that the trust radius also changes during the optimization. In the present method we used the algorithm described by Culot et al. [12] to modify the trust radius, R .

Another important point related to the algorithm is the initiation step. This initiation step is completely similar to that described in Ref. [21]. The geometry parameters of both reactant and product in nonredundant internal coordinates are defined in the same manner. The subset of parameters that show the largest difference between reactant and product are selected as \mathbf{q}_r^0 and the rest of the parameters define the \mathbf{q}_p^0 vector. Normally the dimension of the \mathbf{q}_r^0 vector is 1, 2, or 3. Since both the reactant and the product are stationary points on the PES they cannot be used as initial steps. In this first step the vector \mathbf{q}_r^0 is perturbed by a small amount, $\mathbf{q}_r^0 + \Delta \mathbf{q}_r^0$. At this new perturbed point the gradient vector and the Hessian matrix are computed and the energy is minimized with respect to the \mathbf{q}_p^0 coordinates. The resulting \mathbf{q}_p coordinates together with the $\mathbf{q}_r^0 + \Delta \mathbf{q}_r^0$ coordinates configure the starting point. The resulting geometry with the corresponding gradient vector and Hessian matrix are taken as initial points to start the search process to locate the transition state. Note that the sign of the variation of the $\Delta \mathbf{q}_r^0$ vector depends on the direction of the search, i.e., it depends if one goes from reactant to product or vice versa.

3.2 Algorithm

Now we describe briefly an algorithm based on the results of the previous subsection.

1. With the slightly perturbed geometry parameters from reactant or product, compute the energy, gradient vector, and the Hessian matrix. Note that the gradient vector has the structure $(\mathbf{g}^0)^T = [(\mathbf{g}_r^0)^T, (\mathbf{g}_p^0)^T]$, where $\mathbf{g}_r^0 \neq \mathbf{0}_r$ and $\mathbf{g}_p^0 = \mathbf{0}_p$.
2. With the partitioned blocks of the Hessian matrix, \mathbf{F}_{rr}^0 , \mathbf{F}_{rp}^0 , and \mathbf{F}_{pp}^0 build the reduced or effective Hessian matrix, $\bar{\mathbf{F}}_{rr}^0$, according to Eq. (9) and the metric matrix, \mathbf{S}_{rr}^0 , according to Eq. (25).
3. Build and solve the set of Eqs. (28) and (29). This is done by projecting Eq. (28) on the set of eigenvectors that diagonalizes the $\bar{\mathbf{F}}_{rr}^0$ matrix and the resulting equation is substituted in Eq. (29) obtaining

$$R^2 = \left(\bar{\mathbf{g}}_r^0 \right)^T \mathbf{U}_{rr}^0 \left(\bar{\mathbf{f}}_{rr}^0 - \lambda \mathbf{I}_{rr} \right)^{-2} \left(\mathbf{U}_{rr}^0 \right)^T \bar{\mathbf{g}}_r^0. \quad (30)$$

In Eq. (30) the \mathbf{U}_{rr}^0 matrix contains the eigenvectors and the diagonal matrix $\bar{\mathbf{f}}_{rr}^0$ the eigenvalues of the $\bar{\mathbf{F}}_{rr}^0$ matrix. The solution of Eq. (30) is done by the Hebden procedure [23]. Briefly, the Hebden proce-

ture in nothing more than a Newton–Raphson method for λ to solve Eq. (30). Once time λ parameter has been computed using Eq. (28) the $\Delta\bar{\mathbf{q}}_r^0$ vector is evaluated; finally, using this vector and the $(\mathbf{S}_{rr}^0)^{-1/2}$ matrix the $\Delta\mathbf{q}_r^0$ displacement vector is obtained. λ is selected according to the previous discussion. Using Eq. (17) compute the $\Delta\mathbf{q}_p^0$ displacement vector.

4. With the new geometry compute the corresponding new energy and test the validity of the trust radius [12]. If the trust radius used does not represent the best region for the present quadratic model reject the new point and with the new trust radius go to step 3 to evaluate a new λ parameter and consequently a new geometry displacement vector. Otherwise compute the new gradient and test the convergency criterium. Stop the process if the convergency criterium is fulfilled: the transition state has been reached.
5. With the geometry displacement vector and the gradient variation vector update the Hessian matrix. The Murtagh–Sargent–Powell [28] formula is used to update the Hessian matrix since it has been shown that this formula preserves the nonpositive character of the Hessian matrix [29], which is a basic condition to locate any transition state. The resulting Hessian matrix update is checked using the procedure recently proposed by Eckert and Werner [30].
6. At the new point, normally the corresponding \mathbf{g}_p vector is slightly different from the zero vector, violating the condition of the RPES; consequently a minimization is carried out with respect to the \mathbf{q}_p parameters. During this minimization the \mathbf{q}_r geometry parameters are fixed. Note that in this minimization process the Broyden–Fletcher–Goldfarb–Shanno (BFGS) [23] formula to update the Hessian matrix cannot be used since this Hessian is not positive-definite. In the next subsection we describe a formula to update the Hessian matrix for this special case. When the minimization is finished the new point satisfies the RPES condition, i.e., $\mathbf{g}_r \neq \mathbf{0}_r$ and $\mathbf{g}_p = \mathbf{0}_p$. Then, with this new gradient vector and Hessian matrix go to step 2.

3.3 A Hessian matrix update formula applied to energy minimization with respect to a subset of variables

We are dealing with the problem to minimize the energy with respect to some subset of variables and the rest of the variables are fixed during the minimization process. In addition the full Hessian matrix, \mathbf{F} , is not positive-definite but the Hessian part associated with the nonfixed variables, \mathbf{F}_{pp} , is positive-definite during all the optimization process. During this type of minimization process the full Hessian matrix should preserve these two conditions. Note that in this type of minimization the gradient components associated with the fixed variables change. So far any Hessian matrix update formulae used in minimization algorithms does not satisfy all these requirements since the BFGS formula widely used in minimization algorithms forces all the

Hessian matrix to be positive [23, 31]. However, the \mathbf{F}_{pp} submatrix should be updated by a BFGS-type formula in order to get efficiency in this partial or restricted minimization. Consequently we propose a new Hessian matrix update formula that satisfies all the conditions mentioned earlier; as will see later the resulting formula is very close to the BFGS formula and consequently its behavior will be very similar.

The most general formula to update any type of symmetric Hessian matrix is [29, 32]

$$\mathbf{F} = \mathbf{F}^0 + \Xi_0 \mathbf{u}_0^T + \mathbf{u}_0 \Xi_0^T - (\Xi_0^T \Delta\mathbf{q}_0) \mathbf{u}_0 \mathbf{u}_0^T, \quad (31)$$

where \mathbf{F}^0 is the full Hessian matrix evaluated at \mathbf{q}^0 . If Eq. (31) is applied in a partitioned PES, such as the RPES presented earlier, the components of this formula are defined in the following way:

$$\Xi_0 = \begin{pmatrix} \Xi_r^0 \\ \Xi_p^0 \end{pmatrix} = \begin{pmatrix} \mathbf{g}_r - \mathbf{g}_r^0 \\ \mathbf{g}_p - \mathbf{g}_p^0 \end{pmatrix} - \begin{pmatrix} \mathbf{F}_{rr}^0 & \mathbf{F}_{rp}^0 \\ \mathbf{F}_{pr}^0 & \mathbf{F}_{pp}^0 \end{pmatrix} \begin{pmatrix} \Delta\mathbf{q}_r^0 \\ \Delta\mathbf{q}_p^0 \end{pmatrix}, \quad (32)$$

$$\begin{aligned} \mathbf{u}_0 &= \begin{pmatrix} \mathbf{u}_r^0 \\ \mathbf{u}_p^0 \end{pmatrix} = \frac{\mathbf{M} \Delta\mathbf{q}^0}{(\Delta\mathbf{q}^0)^T \mathbf{M} \Delta\mathbf{q}^0} \\ &= \frac{1}{(\Delta\mathbf{q}^0)^T \mathbf{M} \Delta\mathbf{q}^0} \begin{pmatrix} \mathbf{M}_{rr} & \mathbf{M}_{rp} \\ \mathbf{M}_{pr} & \mathbf{M}_{pp} \end{pmatrix} \begin{pmatrix} \Delta\mathbf{q}_r^0 \\ \Delta\mathbf{q}_p^0 \end{pmatrix}, \end{aligned} \quad (33)$$

where \mathbf{M} is a symmetric and positive-definite matrix. Taking into account the fact that during the minimization process $\Delta\mathbf{q}_r^0 = \mathbf{0}_r$, a possible solution of the problem consists of selecting an \mathbf{M} matrix such that $\mathbf{M}_{rp} = (\mathbf{M}_{pr})^T = \mathbf{0}_{rp}$. With this type of \mathbf{M} matrix $\mathbf{u}_r^0 = \mathbf{0}_r$ and the partitioned form of the update formula given in Eq. (31) takes the following structure

$$\mathbf{F}_{rr} = \mathbf{F}_{rr}^0, \quad (34)$$

$$\mathbf{F}_{rp} = \mathbf{F}_{rp}^0 + \Xi_r^0 (\mathbf{u}_p^0)^T, \quad (35)$$

$$\mathbf{F}_{pr} = \mathbf{F}_{pr}^0 + \mathbf{u}_p^0 (\Xi_r^0)^T, \quad (36)$$

$$\begin{aligned} \mathbf{F}_{pp} &= \mathbf{F}_{pp}^0 + \mathbf{u}_p^0 (\Xi_p^0)^T + \Xi_p^0 (\mathbf{u}_p^0)^T \\ &\quad - \left[(\Delta\mathbf{q}_p^0)^T \Xi_p^0 \right] \mathbf{u}_p^0 (\mathbf{u}_p^0)^T. \end{aligned} \quad (37)$$

In Eqs. (34), (35), (36), and (37) the \mathbf{M}_{rr} submatrix does not appear; only the \mathbf{M}_{pp} submatrix appears through the \mathbf{u}_p^0 vector. Owing to this fact we are only interested in the mathematical structure of the \mathbf{M}_{pp} submatrix. It is very well known that for energy minimizations the BFGS is the best formula to update the Hessian matrix; consequently we select the \mathbf{M}_{pp} submatrix so that we obtain an update formula very close to the BFGS formula. In this case the \mathbf{M}_{pp} matrix takes the following form [31]

$$\mathbf{M}_{pp} = a\mathbf{F}_{pp}^0 + b\mathbf{F}_{pp}^0, \quad (38)$$

where $a + b = 1$ and $a, b \geq 0$ and the matrices \mathbf{F}_{pp}^0 and \mathbf{F}_{pp} are assumed to be positive-definite. With these

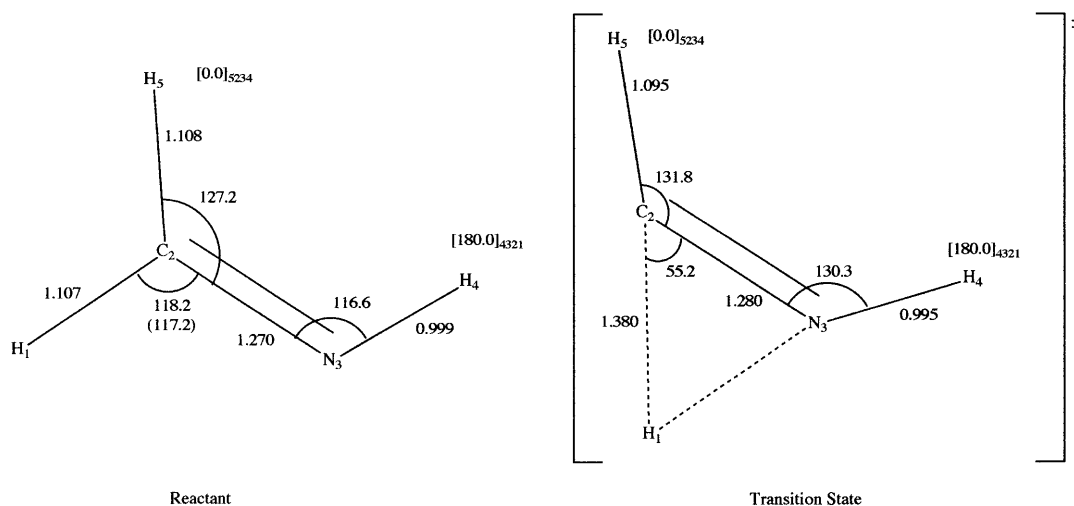


Fig. 1. The geometry parameters of the reactant and transition state (TS) for the isomerization reaction $\text{H}_2\text{CNH} \rightarrow \text{HCNH}_2$. In parentheses the perturbation of the selected “reaction coordinate”, $\text{H}_1\text{C}_2\text{N}_3$ bond angle. The bond lengths are given in angstroms and the bond and dihedral angles in degrees

definitions and the quasi-Newton condition applied on the \mathbf{q}_p variables, $\mathbf{F}_{pp}^0 \Delta \mathbf{q}_p^0 = \mathbf{g}_p - \mathbf{g}_p^0$, the \mathbf{u}_p^0 vector is

$$\mathbf{u}_p^0 = \frac{a(\mathbf{g}_p - \mathbf{g}_p^0) + b\mathbf{F}_{pp}^0 \Delta \mathbf{q}_p^0}{a(\Delta \mathbf{q}_p^0)^T (\mathbf{g}_p - \mathbf{g}_p^0) + b(\Delta \mathbf{q}_p^0)^T \mathbf{F}_{pp}^0 \Delta \mathbf{q}_p^0} \quad (39)$$

The scalars a and b are not computed in the usual way [31]: they are evaluated according to the following formulae

$$a = \frac{\left[(\mathbf{g}_p - \mathbf{g}_p^0)^T \Delta \mathbf{q}_p^0 \right]^2}{(\mathbf{g}_p - \mathbf{g}_p^0)^T (\mathbf{g}_p - \mathbf{g}_p^0) (\Delta \mathbf{q}_p^0)^T \Delta \mathbf{q}_p^0}, \quad (40)$$

$$b = 1 - a. \quad (41)$$

The resulting update for the \mathbf{F}_{pp} matrix is very close to that obtained using the BFGS formula.

4 Examples and analysis

The algorithm described in the preceding section was implemented in a modified version of the MOPAC program [33, 34]. The transition-state searches of all the chemical reactions described here were calculated using the corresponding wavefunction and the Austin model 1 (AM1) [35] semiempirical Hamiltonian. The convergence criterion was on the maximum component of the gradient vector, $10^{-3} \text{ kcal mol}^{-1} \text{ \AA}^{-1} - \text{kcal mol}^{-1} \text{ rad}^{-1}$. The initial perturbation vector, $\Delta \mathbf{q}_r$, of the first step was 0.1 \AA for bond lengths and 1.0° for bond and dihedral angles. Following Eckert and Werner [30], if the root-mean-square deviation of the Hessian matrix before and after update is larger than $0.5 \text{ kcal mol}^{-1} \text{ \AA}^{-2} - \text{kcal mol}^{-1} \text{ \AA}^{-1} \text{ rad}^{-1} - \text{kcal mol}^{-1} \text{ rad}^{-2}$ then the Hessian matrix is computed in a normal way rather than updated.

4.1 The isomerization reaction $\text{H}_2\text{CNH} \rightarrow \text{HCNH}_2$

This reaction was studied by Andzelm et al. [36] using density functional theory; however, we present the results of this reaction using the AM1 model within the C_s point group of symmetry. The initial perturbed and nonperturbed reactant geometry and the final transition-state molecular geometry are shown in Fig. 1. The selected “reaction coordinate” corresponds to the bond angle $\text{H}_1\text{C}_2\text{N}_3$; the rest of the geometry parameters are the set of coordinates that are “equilibrium-adapted” during the process. The method reaches the desired transition state within 16 iterations or steps. The behavior of the heat of formation and the maximum component of the gradient vector during the search process is presented in Fig. 2. We note that from

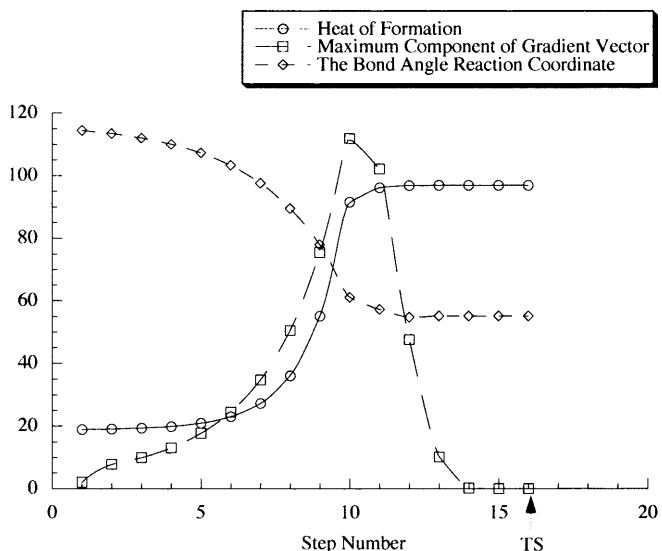


Fig. 2. The evolution of the heat of formation, the maximum component of the gradient vector, and the “reaction coordinate” $\text{H}_1\text{C}_2\text{N}_3$ bond angle with respect to the steps of the location process of the TS for the isomerization reaction $\text{H}_2\text{CNH} \rightarrow \text{HCNH}_2$ according to the proposed method. The heat of formation is given in kcal mol^{-1} , the gradient component in $\text{kcal mol}^{-1} \text{ \AA}^{-1} - \text{kcal mol}^{-1} \text{ rad}^{-1}$, and the bond angle in degrees

iteration 8–10 the heat of formation also presents a strong variation at the steps the gradient vector presents the largest maximum component. It is interesting to note that after iteration 10 the reduced or effective Hessian matrix, given in Eq. (9), shows a negative eigenvalue. Also in Fig. 2 we show how the “reaction coordinate” changes during the search process: the $\text{H}_1\text{C}_2\text{N}_3$ bond angle takes practically the transition-state value after iteration 10.

Now we compare the behavior of the present algorithm with the algorithm described in Ref. [21], which briefly consists of reaching a transition state following a type of steepest ascent–descent path. The behavior of the

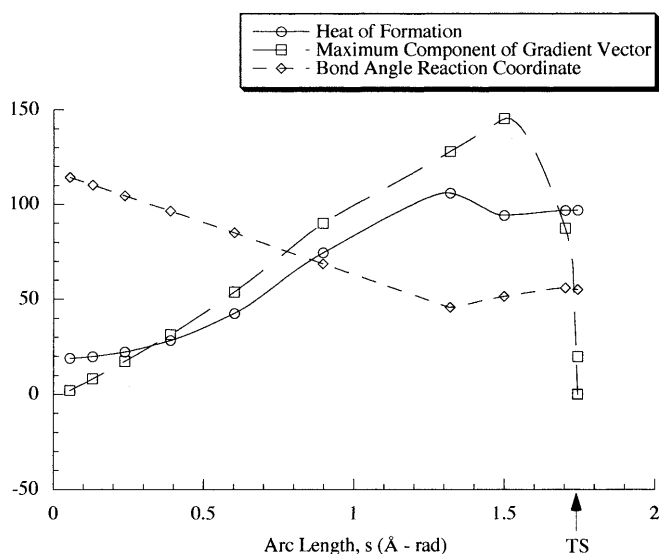


Fig. 3. The evolution of the heat of formation, the maximum component of the gradient vector, and the “reaction coordinate” $\text{H}_1\text{C}_2\text{N}_3$ bond angle with respect to the arc length for the location process of the TS for the isomerization reaction $\text{H}_2\text{CNH} \rightarrow \text{HCNH}_2$ according to the method proposed in Ref. [21]. The heat of formation is given in kcal mol^{-1} , the gradient component in $\text{kcal mol}^{-1} \text{Å}^{-1} - \text{kcal mol}^{-1} \text{rad}^{-1}$, and the bond angle in degrees

heat of formation, that of the maximum component of the gradient vector, and that of the $\text{H}_1\text{C}_2\text{N}_3$ bond angle with respect to the arc length of the path, s , are shown in Fig. 3. We observe that for $1.3 \leq s \leq 1.5$, both the heat of formation and the maximum component of the gradient vector take the largest value. At $s = 1.5$, the reduced or effective Hessian matrix presents a change of sign from positive to negative. Finally, comparing Figs. 2 and 3 we see that the $\text{H}_1\text{C}_2\text{N}_3$ bond angle takes different values for each curve. This means that the path of the present algorithm and that described in Ref. [21] are different.

4.2 Ring closure of vinylketene rearrangement

A detailed theoretical study of this reaction was reported by Nguyen et al. [37] at the ab initio level of theory. The location of the transition state using the proposed method was done by employing the AM1 semiempirical Hamiltonian. The molecular geometry parameters of *cis*-vinylketene and the transition state are shown in Fig. 4. The C_2C_8 bond length and the $\text{H}_9\text{C}_8\text{C}_6\text{C}_4$ dihedral angle were selected as “reaction coordinate” parameters. The initial values for these two parameters are given in parentheses in Fig. 4. Note that the corresponding initial perturbation for these two parameters is very small and the sense of this perturbation is that it goes from vinylketene to cyclobutenone. The behavior of the heat of formation and that of the maximum component of the gradient vector during the location of the transition state are shown in Fig. 5. The largest value of the maximum component of the gradient vector is reached at iteration 12. On the other hand, the heat of formation varies from the first iteration to iteration 28: at this step the algorithm reaches the converged value. During the location process of the transition state, the reduced or effective Hessian matrix achieves a negative eigenvalue at iteration 15. Finally, in Fig. 5, we present the variations of the two “reaction coordinates” during the search process; these two “reaction coordinates” are

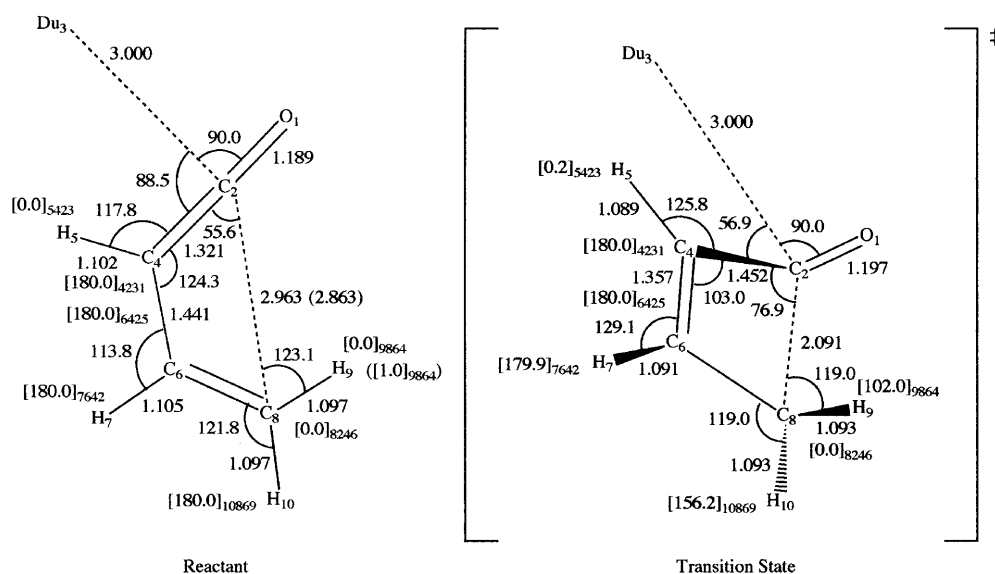


Fig. 4. The geometry parameters of the reactant and TS for the ring closure of the vinylketene rearrangement. In parentheses the perturbation of the selected “reaction coordinates”, C_2C_8 bond length and $\text{H}_9\text{C}_8\text{C}_6\text{C}_4$ dihedral angle. The bond lengths are given in angstroms and the bond and dihedral angles in degrees

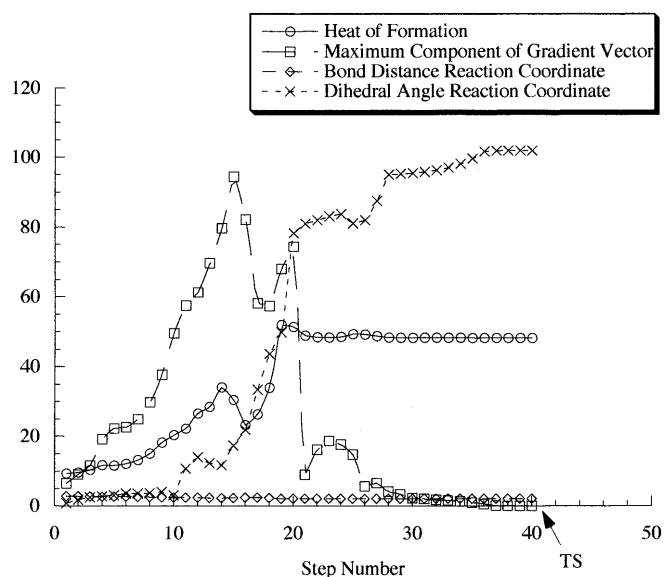


Fig. 5. The evolution of the heat of formation, the maximum component of the gradient vector, and the “reaction coordinates” C_2C_8 bond length and $H_9C_8C_6C_4$ dihedral angle with respect to the steps of the location process of the TS for the ring closure of the vinylketene rearrangement according to the proposed method. The heat of formation is given in kcal mol⁻¹, the gradient component in kcal mol⁻¹ Å⁻¹ – kcal mol⁻¹ rad⁻¹, the bond distance in Å, and the dihedral angle in degrees

labeled as the bond length reaction coordinate for the C_2C_8 bond length and the dihedral angle reaction coordinate for the $H_9C_8C_6C_4$ dihedral angle. The C_2C_8 bond length achieves the value of the transition state at iteration 33 and the $H_9C_8C_6C_4$ dihedral angle is stabilized at step 36. Owing to the scale reduction in Fig. 5 is not possible to appreciate the variation of the C_2C_8 bond length; however, it changes from 2.85 Å at the reactant to 2.10 Å at the transition state.

The variations of the heat of formation, the maximum component of the gradient vector, and the “reaction coordinates” of the C_2C_8 bond length and the $H_9C_8C_6C_4$ dihedral angle with respect to the arc length, s , using the method described in Ref. [21] are shown in Fig. 6. By comparing this figure with Fig. 5, we conclude that both the present algorithm and that described in Ref. [21] use different paths to reach the transition state.

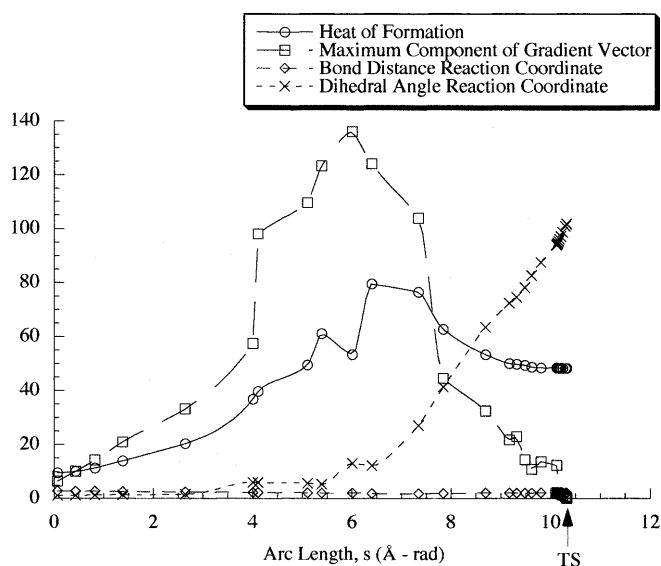
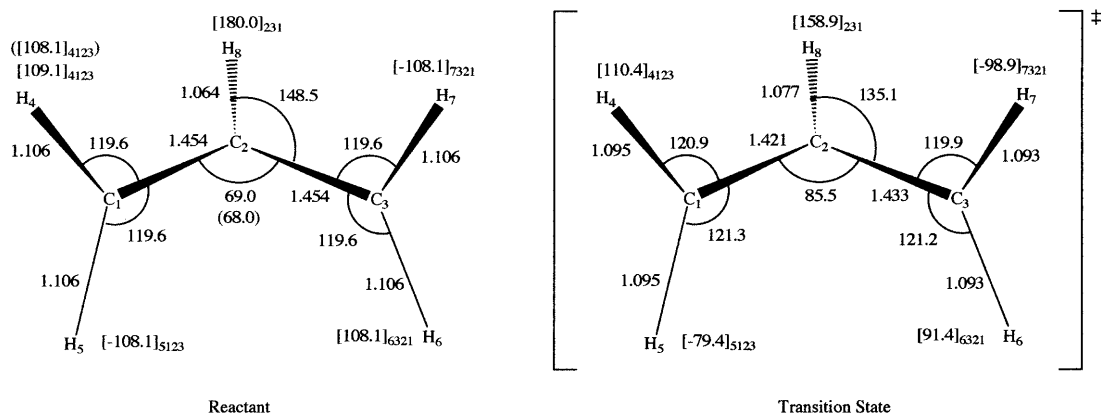


Fig. 6. The evolution of the heat of formation, the maximum component of the gradient vector, and the “reaction coordinates” C_2C_8 bond length and $H_9C_8C_6C_4$ dihedral angle with respect to the arc length for the location process of the TS for the ring closure of the vinylketene rearrangement according to the method proposed in Ref. [21]. The heat of formation is given in kcal mol⁻¹, the gradient component in kcal mol⁻¹ Å⁻¹ – kcal mol⁻¹ rad⁻¹, the bond length in Å, and the dihedral angle in degrees

4.3 Ring opening of cyclopropyl radical rearrangement

This reaction was studied by Olivella et al. [38] at the ab initio level of theory. We locate the transition state by using the AM1 semiempirical Hamiltonian and the proposed method. The molecular geometry parameters of the reactant, the slightly perturbed reactant, and the located transition state are shown in Fig. 7. The variation of the heat of formation and the maximum component of the gradient vector in the location process of the transition state are given in Fig. 8. In order to locate the transition state two geometry parameters were

Fig. 7. The geometry parameters of the reactant and TS for the ring opening of cyclopropyl radical rearrangement. In *parentheses* the perturbation of the selected “reaction coordinates” $C_1C_2C_3$ bond angle and $H_4C_1C_2C_3$ dihedral angle. The bond lengths are given in angstroms and the bond and dihedral angles in degrees



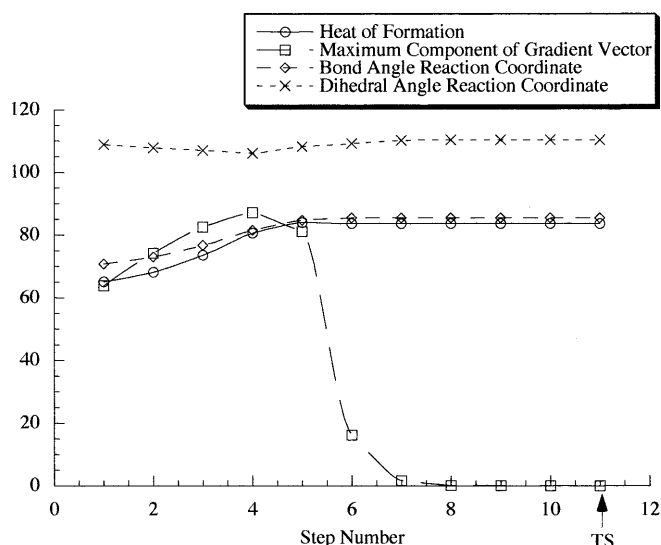


Fig. 8. The evolution of the heat of formation, the maximum component of the gradient vector, and the “reaction coordinates” $C_1C_2C_3$ bond angle and $H_4C_1C_2C_3$ dihedral angle with respect to the steps of the location process of the TS for the ring opening of cyclopropyl radical rearrangement according to the proposed method. The heat of formation is given in kcal mol^{-1} , the gradient component in $\text{kcal mol}^{-1} \text{Å}^{-1} - \text{kcal mol}^{-1} \text{rad}^{-1}$, the bond angle and the dihedral angle in degrees

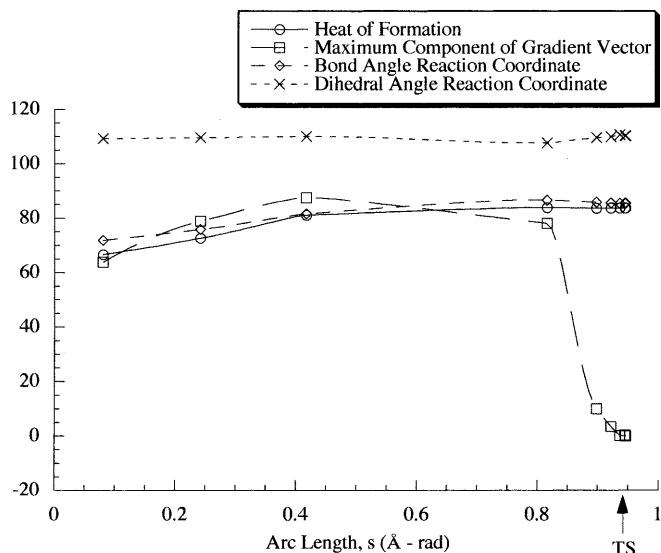


Fig. 9. The evolution of the heat of formation, the maximum component of the gradient vector, and the “reaction coordinates” $C_1C_2C_3$ bond angle and $H_4C_1C_2C_3$ dihedral angle with respect to the arc length for the location process of the TS for the ring opening of cyclopropyl radical rearrangement according to the method proposed in Ref. [21]. The heat of formation is given in kcal mol^{-1} , the gradient component in $\text{kcal mol}^{-1} \text{Å}^{-1} - \text{kcal mol}^{-1} \text{rad}^{-1}$, the bond angle and the dihedral angle in degrees

used as a “reaction coordinates”; namely, the $C_1C_2C_3$ bond angle and the $H_4C_1C_2C_3$ dihedral angle. The behavior of these two geometry parameters during the location process is also presented in Fig. 8. The heat of formation is stabilized after step 5. The reduced or

effective Hessian matrix possesses a negative eigenvalue after step 4.

In order to compare the present method with that described in Ref. [21], we show the behavior of the heat of formation, the maximum component of the gradient vector, and the “reaction coordinates” $C_1C_2C_3$ bond angle and the $H_4C_1C_2C_3$ dihedral angle with respect to the arc length, s , according to that algorithm [21] in Fig. 9. As in the previous examples, both algorithms converge to the same transition state; however, the paths are different.

5 Conclusions

We have proposed a method to locate transition states starting from both slightly perturbed geometry reactants or products. The search is carried out on a RPES defined by the subset of variables labeled “reaction coordinate”; the rest of variables are minimized with respect to the energy. The method converges to the transition state normally within a reasonable number of steps. From the behavior of the present method compared with that proposed in Ref. [21] we say that they are very similar; however, they define different paths to walk from the minimum to the transition state.

Acknowledgements. We are indebted to S. Olivella for his valuable suggestions. We give thanks to the unknown referee for valuable suggestions. This research was supported by the Spanish DGICYT (grants PB98-1240-C02-01 and PB98-1240-C02-02).

References

1. Truhlar DG, Garret BC, Klippenstein SJ (1996) *J Phys Chem* 100: 12771
2. Schlegel HB (1995) In: Yarkony DR (ed) *Modern electronic structure theory*. World Scientific, Singapore pp 459–500
3. Panciř J (1975) *Collect Czech Chem Commun* 40: 1112
4. Cerjan CJ, Miller WH (1981) *J Chem Phys* 75: 2800
5. Basilevsky MV, Shamov AG (1981) *Chem Phys* 60: 347
6. Simons J, Jørgensen P, Taylor H, Ozment J (1983) *J Phys Chem* 87: 2745
7. Banerjee A, Adams N, Simons J, Shepard R (1985) *J Phys Chem* 89: 52
8. Baker J (1986) *J Comput Chem* 7: 385
9. Nichols J, Taylor H, Schmidt P, Simons J (1990) *J Chem Phys* 92: 340
10. Smith CM (1990) *Int J Quantum Chem* 37: 773
11. Helgaker T (1991) *Chem Phys Lett* 182: 503
12. Culot P, Dive G, Nguyen VH, Ghuysen JM (1992) *Theor Chim Acta* 82: 189
13. Besalú E, Bofill JM (1998) *Theor Chem Acc* 100: 265
14. Czerminski R, Elber R (1990) *J Chem Phys* 92: 5580
15. Mathias P, Sanders WA (1976) *J Chem Phys* 64: 3898
16. Muller K (1980) *Angew Chem Int Ed Engl* 19: 1
17. Rothman MJ, Lohr LL Jr (1980) *Chem Phys Lett* 70: 405
18. Scharfenberg P (1982) *J Comput Chem* 3: 277
19. Williams IH, Maggiora GM (1982) *J Mol Struct (THEOCHEM)* 89: 365
20. Quapp W, Hirsch M, Heidrich D (1998) *Theor Chem Acc* 100: 285
21. Anglada JM, Besalú E, Bofill JM, Crehuet R (2001) *J Comput Chem* 22: 387
22. Scharfenberg P (1981) *Chem Phys Lett* 79: 115

23. Fletcher R (1987) Practical methods of optimization, Wiley, New York
24. Parlett BN (1980) The symmetry eigenvalue problem, Prentice Hall, New Jersey
25. Olsen J, Jørgensen P, Yeager DL (1982) J Chem Phys 76: 527
26. Shepard R, Shavitt R, Simons J (1982) J Chem Phys 76: 543
27. Khait YG, Panin AI, Averyanov AS (1995) Int J Quantum Chem 54: 329
28. Bofill JM (1994) J Comput Chem 15: 1
29. Bofill JM, Comajuan M (1995) J Comput Chem 16: 1326
30. Eckert F, Werner HJ (1998) Theor Chem Acc 100: 21
31. Anglada JM, Bofill JM (1998) J Comput Chem 19: 349
32. Greenstadt J (1970) Math Comput 24: 1
33. Stewart JJP (1983) QCPE Bull 3: 101
34. Olivella S (1984) QCPE Bull 4: 109
35. Dewar MJS, Zoebisch EG, Healy EF, Stewart JJP (1985) J Am Chem Soc 107: 3902
36. Andzelm J, Baker J, Scheiner AC, Wrinn M (1995) Int J Quantum Chem 56: 733
37. Nguyen MT, Ha TK, More O'Ferrall RA (1990) J Org Chem 55: 3251
38. Olivella S, Solé A, Bofill JM (1990) J Am Chem Soc 112: 2160